Am J Cancer Res 2024;14(12):5965-5986
www.ajcr.us /ISSN:2156-6976/ajcr0161470

Original Article

A novel semi-quantitative scoring method for CD8+ tumor-infiltrating lymphocytes based on infiltration sites in gastric cancer

Yudai Nakabayashi[1*], Jun Kiuchi[1*], Takeshi Kubota[1], Takuma Ohashi[1], Keiji Nishibeppu[1], Taisuke Imamura[1], Kenji Nanishi[1], Hiroki Shimizu[1], Tomohiro Arita[1], Yusuke Yamamoto[1], Hirotaka Konishi[1], Ryo Morimura[1], Shuhei Komatsu[1], Atsushi Shiozaki[1], Hisashi Ikoma[1], Yoshiaki Kuriu[1], Hitoshi Fujiwara[1], Hitoshi Tsuda[2], Eigo Otsuji[1]

[1]Division of Digestive Surgery, Department of Surgery, Kyoto Prefectural University of Medicine, Kawaramachi-Hirokoji, Kamigyo-ku, Kyoto, Japan; [2]Department of Basic Pathology, National Defense Medical College, Tokorozawa, Japan. [*]Equal contributors.

Received October 25, 2024; Accepted December 18, 2024; Epub December 25, 2024; Published December 30, 2024

Abstract: No established method currently exists for evaluating tumor-infiltrating lymphocytes (TILs) in gastric cancer (GC), and their clinical significance based on infiltration site in GC remains unclear. In this study, we developed a method to evaluate TILs according to their infiltration site as a prognostic marker for GC. We retrospectively analyzed 103 patients with advanced GC who underwent curative resection. TILs located at the invasive margin (TIL_{IM}) and the center of tumors (TIL_{CT}) were scored semi-quantitatively using immunohistochemical staining of CD8+ T cells. The sum of the TIL_{IM} and TIL_{CT} scores was defined as the TILs score. Based on this score, patients were classified into low and high TILs groups. Quantitative TILs were also assessed to validate the semi-quantitative scoring method. Furthermore, we confirmed a tumor suppressive effect due to CD8+ T cells co-cultured in GC cell lines *in vitro*. In the univariate analysis, patients with low TIL_{IM} were significantly more likely to be female, younger, and have undifferentiated histological types and deeper tumor invasion compared to those with high TIL_{IM}. Similarly, patients with low TIL_{CT} had significantly more positive lymph node metastases than those with high TIL_{CT}. In the multivariate analysis, deeper tumor invasion and positive lymph node metastasis were identified as independent risk factors for patients with low TIL_{IM} and low TIL_{CT}, respectively. According to our semi-quantitative TILs scoring method, the low TILs group had significantly poorer prognoses compared to the high TILs group. This group had significantly larger tumor diameters, deeper tumor invasion, and more positive lymph node metastases. Additionally, deeper tumor invasion was an independent risk factor for the low TILs group. Quantitative TILs analysis revealed that the low TILs group had significantly lower TIL levels compared to the high TILs group. *In vitro*, CD8+ T cells induced apoptosis in GC cells in a concentration-dependent manner. Furthermore, these cells significantly suppressed the proliferative, migratory, and invasive capacities of GC cells. Our simple and versatile semi-quantitative scoring method for CD8+ TILs indicates that CD8+ TILs are sensitive prognostic markers. The low TILs group accurately reflects the low quantitative TIL levels and is associated with poor oncological prognosis.

Keywords: CD8+ T cells, gastric cancer, immunohistochemical staining, semi-quantitative scoring, tumor-infiltrating lymphocytes

Introduction

Gastric cancer (GC) is one of the most common causes of cancer-related deaths worldwide [1]. Following curative gastrectomy, disease recurrence poses a significant risk for all patients with GC. Indeed, nearly 20% of patients with advanced GC experience recurrence after surgery [2]. Therefore, it is necessary to explore biomarkers that can predict which patients are most at risk of recurrence and would thus benefit the most from early treatment of GC.

Tumor-infiltrating lymphocytes (TILs) reflect local tumor immunity and have been shown to predict improved prognosis in various cancers [3-5]. TILs include various types of immune cells, such as cytotoxic T cells, helper T cells

https://doi.org/10.62347/JKCU5881

and natural killer cells, which contribute to anti-tumor responses. Conversely, other cells, such as FOXP3 regulatory T (Treg) cells, have a pro-tumorigenic effect that promotes cancer growth and invasion by producing factors that sustain angiogenesis and promote cancer cell proliferation [6, 7]. CD8+ T cells, classified as cytotoxic T cells, release cytokines that promote cytotoxicity, and directly inhibit tumor growth [7, 8]. Therefore, it is important to evaluate the role of CD8+ TILs in tumor immunity. However, there is a crucial issue that must be resolved before TILs can be clinically applied for the treatment of GC. The clinical significance of TILs based on their infiltration site in GC remains unclear. Furthermore, no standardized method for evaluating the role of TILs in GC has been established, and there is insufficient robust evidence regarding the significance of TILs in GC.

In this study, therefore, we investigated a method to evaluate CD8+ TILs based on their infiltration site as a prognostic marker for GC, using clinical GC specimens, and analyzed their clinical significance. Additionally, we confirmed the tumor-suppressive effect of different concentrations of CD8+ T cells by co-culturing them with GC cell lines *in vitro*.

Materials and methods

Ethics approval and consent to participate

This study was approved by the institutional review board of Kyoto Prefectural University of Medicine (ERB-C-1178) on June 12, 2018. All experimental methods were carried out in accordance with relevant guidelines, such as the Declaration of Helsinki and REMARK guidelines. Written informed consent was obtained from all patients to use their clinical data and tissue specimens.

Patients and surgical procedures

Paraffin-embedded primary GC tissue samples were collected from 103 patients with GC who had undergone curative gastrectomy (R0) between 2011 and 2014, at the Division of Digestive Surgery, Kyoto Prefectural University of Medicine, and whose pathological diagnosis showed tumors present that were deeper than the submucosal layer. None of these patients had received prior treatment such as neoadjuvant chemotherapy or radiotherapy. Curative resection was performed as a distal or total gastrectomy, depending on the location of the tumor, to obtain a tumor-free resection margin, and radical lymphadenectomy was performed according to the Japanese Gastric Cancer Treatment Guidelines [9]. Resected specimens were examined by two or more pathologists according to the 15th Japanese Classification of Gastric Carcinomas (JCGC) and the 8th Tumor-Node-Metastasis (TNM) classifications [10, 11]. The clinicopathological findings for these patients were retrospectively determined from their hospital records.

Postoperative follow-up and treatment

The follow-up program scheduled for all patients comprised a regular physical examination and laboratory blood tests, including tests for the tumor markers CEA and CA19-9, and chest X-rays every three months in the first postoperative year, every six months in the second postoperative year and annually thereafter for at least five years. Computed tomography was performed annually for patients with tumors of pathological stage I and every six months for patients with tumors of pathological stage II or greater, for the first five years. Otherwise, computed tomography was performed within one month if elevated tumor markers or symptoms were detected by follow-up laboratory blood tests or during regular physical examinations. Endoscopy was performed for all patients annually to screen for cancer in the gastric remnant. Patients with stage II/III GC received adjuvant chemotherapy within 6 weeks of their surgery, according to the Japanese Gastric Cancer Treatment Guidelines [9].

Evaluation of TILs in advanced GC by immunohistochemistry staining

Paraffin-embedded primary GC tissue samples were cut into 5-μm-thick sections and subjected to immunohistochemical staining for CD8+ T cells using the avidin-biotin-peroxidase complex method [12]. The antibodies used were mouse monoclonal anti-CD8 alpha antibodies (C8/144B; Abcam, Tokyo, Japan). Briefly, after deparaffinization, endogenous peroxidases were quenched by incubating the sections in 3% H_2O_2 for 30 min. Antigen retrieval was performed by heating the samples in 10 mmol/L citrate buffer (pH 6.0) at 95°C for 60 min. After treatment with Block Ace (Vectastain Universal

Elite ABC kit; Vector Laboratories, Burlingame, CA) at room temperature for 30 min, the sections were incubated at room temperature for 60 min and at 4°C overnight with anti-CD8 alpha antibodies (1:200). The avidin-biotin-peroxidase complex system (Vectastain Universal Elite ABC kit; Vector Laboratories, Burlingame, CA) was used for color development with diaminobenzidine tetrahydrochloride. The slides were counterstained with Mayer's hematoxylin.

To image the entire GC sample with immunohistochemistry staining of CD8+ T cells, the sections were imaged under an all-in-one fluorescence microscope (BZ-X800; KEYENCE, Osaka, Japan) equipped with a BZ-X800 Analyzer (BZ-H4A; KEYENCE, Osaka, Japan). A Plan Fluor 10× objective (NA0.30, MRH20101; KEYENCE, Osaka, Japan) was used to capture tiled images, and the image stitching function in the BZ-X800 Analyzer software (BZ-H4A; KEYENCE, Osaka, Japan) was used for image stitching (**Figure 1A**) [13, 14].

The tumor area was divided into the invasive margin (IM) and the center of the tumor (CT) within the tumor stroma, according to previously described methods [15-17]. The IM is defined as a 1-mm-wide zone centered around the border of the malignant cells with the host tissue, and the CT is defined as the tumor tissue surrounded by this zone. In some cases, the cancer invades the serosa, and the IM is less than 1 mm wide. In such cases, the serosa is defined as the boundary of the IM. These procedures follow the standardized method proposed by the International Immuno-Oncology Biomarkers Working Group (**Figure 1B**) [18]. Stromal TILs in the IM (TIL_{IM}) and TILs in the CT (TIL_{CT}) were evaluated based on the sites where CD8+ TILs infiltrate. Additionally, intra-tumoral TILs as non-stromal TILs within the tumor nests (TIL_{N}) were assessed in a test-scale group of patients with advanced GC. Prior to the semi-quantitative evaluation of CD8+ TILs, a quantitative evaluation was performed for verification using the Hybrid Cell Count software module of the BZ-X800 Analyzer software. For each GC sample, three regions of the IM and CT, where high densities of CD8+ T cells were observed, were selected. The number of CD8+ T cells (visualized as red) per field of view was counted, and the average value was calculated (**Figure 1C**) [14, 19]. Areas with lymphoid follicles and necrosis were excluded, in accordance with the standardized method proposed by the International Immuno-Oncology Biomarkers Working Group [18]. The value in the IM was defined as quantitative TIL_{IM}, whereas the value in the CT was defined as quantitative TIL_{CT}. The sum of quantitative TIL_{IM} and TIL_{CT} in GC was defined as the total quantitative TILs. The cut-off of values for quantitative TIL_{IM}, TIL_{CT}, and TILs were set at their respective medians.

TIL_{IM} of GC were semi-quantitatively evaluated per low-power field (×100) and TIL_{CT} of GC were semi-quantitatively evaluated per high-power field (HPF) (×400). In both cases, this was carried out by an experienced pathologist. TIL_{IM} were classified from 0 to 3+, as follows (**Figure 1D-G**); 0, none or very few immunopositive lymphocytes; 1+, a few immunopositive lymphocytes; 2+, several immunopositive lymphocytes, seen to be forming a belt; 3+, many immunopositive lymphocytes, seen as a thick belt. TIL_{CT} were also classified from 0 to 3+, as follows (**Figure 1H-K**); 0, none or very few immunopositive lymphocytes; 1+, a low density of immunopositive lymphocytes; 2+, an intermediate density of immunopositive lymphocytes; 3+, a high density of immunopositive lymphocytes. Patients with TIL_{IM} scored as 1 or less were classified as low TIL_{IM}, while those with TIL_{IM} scored as higher than 1 were classified as high TIL_{IM}. TIL_{CT} was classified in the same way. The sum of each TIL_{IM} and TIL_{CT} score was defined as the TILs score. The median TILs score was 3, therefore patients with a TILs score of 3 or less were classified as the low TILs group, and those with a TILs score higher than 3 were classified as the high TILs group.

Cell lines

Two GC cell lines (HGC27 from metastatic lymph nodes and MKN45 from poorly differentiated adenocarcinoma) were used in this study. These cell lines were purchased from RIKEN Cell Bank (Tsukuba, Japan), the Japanese Collection of Research Bioresources Cell Bank (Osaka, Japan) and Cell Lines Service (Eppelheim, Germany). All cell lines were identified by short tandem repeat profiling. No mycoplasma contamination was detected in any of the cultures. HGC27 was cultured in Dulbecco's Minimum Essential Medium (Sigma, St. Louis, MO). MKN45 was cultured in Roswell Park Memorial Institute 1640 medium (Sigma, St. Louis, MO). All media were supplemented with 10% fetal bovine serum (Trace Scientific, Melbourne, Australia). The cells were cultured at

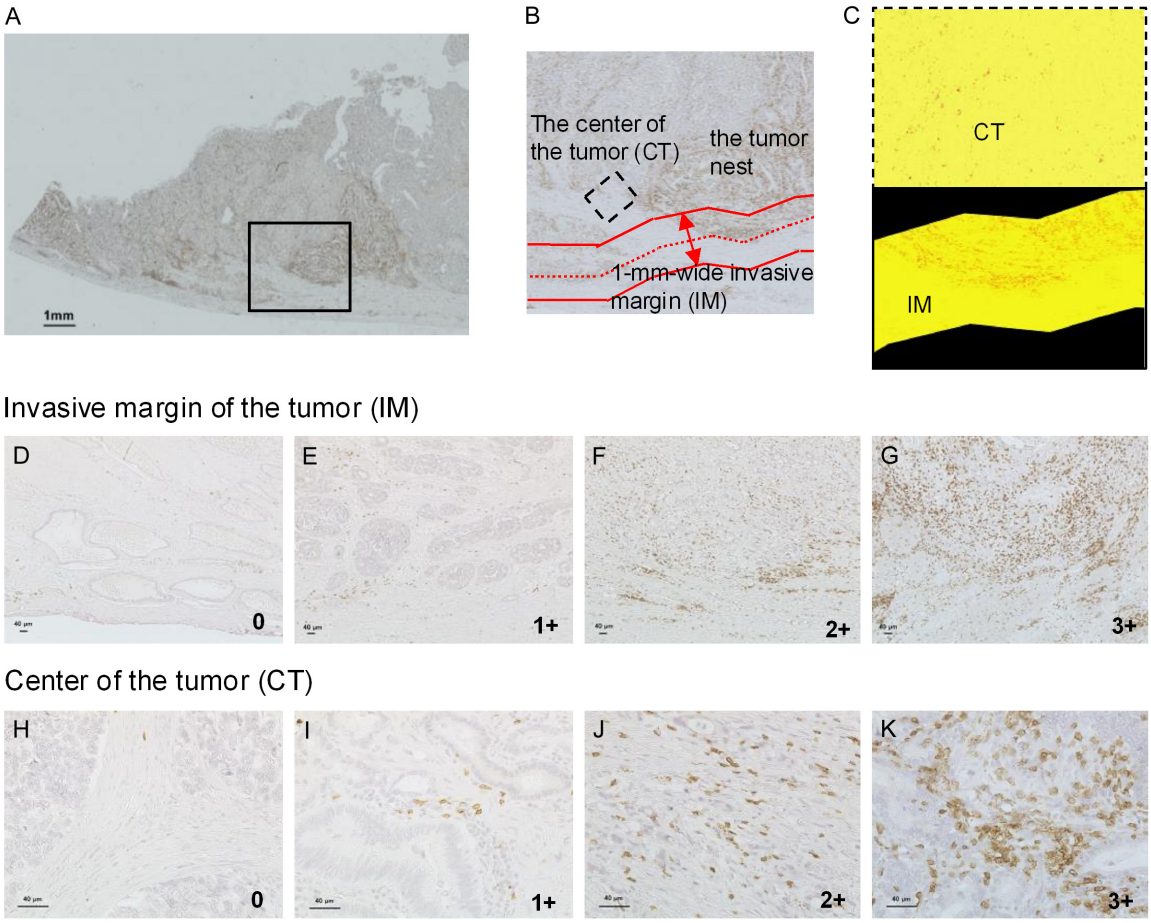

Figure 1. (A) To image the entire gastric cancer (GC) specimen with immunohistochemistry staining of CD8+ T cells, tiled images captured per low-power field (LPF) (×100) were stitched. (B) Enlarged image of the area inside the black rectangle shown in (A). The tumor area was divided into the invasive margin (IM) and the center of the tumor (CT) within the tumor stroma in GC. (C) Representative quantified images of CD8+ tumor-infiltrating lymphocytes (TILs) in the IM and CT of GC are shown. The upper image is the enlarged image of the area inside the black dashed rectangle in the CT shown in (B) where TILs with a high density of CD8+ T cells were observed in the CT. The below image is enlarged image of the area in the IM shown in (B) where TILs with a high density of CD8+ T cells were observed in the IM. CD8+ T cells are indicated in red, and other areas are indicated in yellow. (D-K) Representative cases of semi-quantitative evaluation of stromal TILs are shown. CD8+ TILs in the IM of GC were classified as follows per LPF (×100): 0, none or a very few immunopositive lymphocytes (D); 1+, a few immunopositive lymphocytes (E); 2+, several immunopositive lymphocytes, as indicated by the formation of a belt (F); and 3+, many immunopositive lymphocytes, as indicated by the formation of a thick belt (G). CD8+ TILs in the CT of GC were classified as follows per high-power field (HPF) (×400): 0, none or a very few immunopositive lymphocytes (H); 1+, low density of immunopositive lymphocytes (I); 2+, intermediate density of immunopositive lymphocytes (J); and 3+, high density of immunopositive lymphocytes (K).

37°C in a humidified chamber in a 5% CO_2 incubator.

Isolation and activation of CD8+ T cells

Human peripheral blood mononuclear cells (PBMCs) were isolated from healthy donors' blood using SepMate™-50 (RUO) (STEMCELL Technologies, Cambridge, UK). CD8+ T cells were isolated from PBMCs using the EasySep™ Human CD8+ T cell isolation kit (STEMCELL Technologies, Cambridge, UK), according to the manufacturer's protocol. The purity of the CD8+ T cells was confirmed by flow cytometry before and after isolation. Isolated CD8+ T cells were propagated in Immunocult™-XF T cell expansion medium (STEMCELL Technologies, Cambridge, UK) containing 30-100 IU/mL of recombinant human IL-2 (Peprotech, NJ) and 25 μL/mL of Immunocult™ human CD3/CD28 T cell activator (STEMCELL Technologies, Cambridge, UK), which contained anti-CD3 and anti-

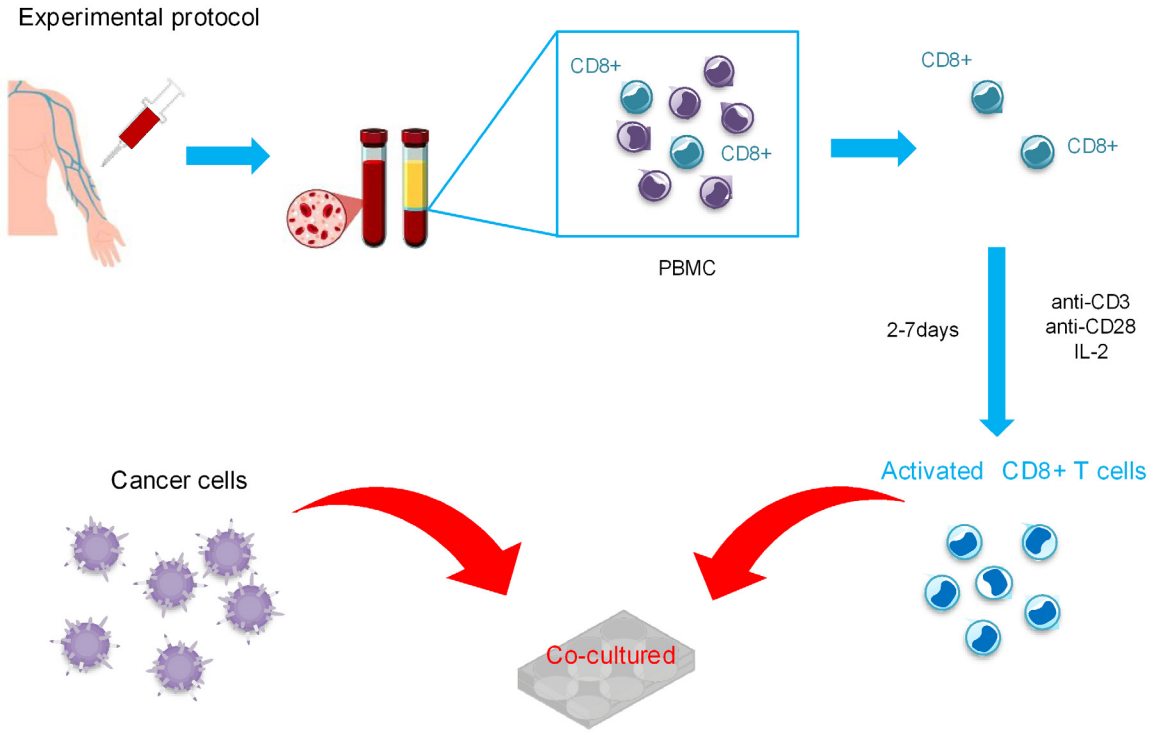

Figure 2. Experimental protocol. Human peripheral blood mononuclear cells (PBMCs) were isolated from healthy donors' blood, and CD8+ T cells were isolated from the PBMCs. Isolated CD8+ T cells were propagated in T cell expansion medium containing 30-100 IU/mL of recombinant human IL-2 and 25 μL/mL of anti-CD3 and anti-CD28 antibodies, at 37°C in a humidified chamber in a 5% CO_2 incubator for 2-7 days.

CD28 antibodies, at 37°C in a humidified chamber in a 5% CO_2 incubator for 2-7 days (**Figure 2**) [20, 21].

Cell growth assays

HGC27 and MKN45 cells, as target cells, were seeded into 24-well plates. The activated CD8+ T cells, as effector cells, were co-cultured in each well with cancer cells at a ratio of 8:1, 0.5:1, and with phosphate-buffered saline (PBS) as a control. To measure cell growth, the number of viable cells at various time points during co-culturing was assessed using a colorimetric water-soluble tetrazolium salt assay (Cell Counting Kit 8; Dojindo Laboratories, Kumamoto, Japan). The CD8+ T cells were washed twice with PBS, and the target cell viability was determined by reading the optical density at 450 nm (Multiskan Fc; Thermo Fisher Scientific, MA).

Apoptotic cell assays

HGC27 and MKN45 cells, as target cells, were seeded into 6-well plates. The activated CD8+ T cells, as effector cells, were co-cultured in each well with cancer cells at a ratio of 8:1, 0.5:1, and with PBS as a control. After co-culturing for 72 h, the CD8+ T cells were washed twice with PBS and the target cells (HGC27 or MKN45) were harvested and stained with fluorescein isothiocyanate-conjugated annexin V and phosphatidylinositol, using an Annexin V Kit (Beckman Coulter, Brea, CA). A Becton Dickinson Accuri™ C6 flow cytometer (Becton Dickinson, San Jose, CA) was used to analyze the proportion of apoptotic cells. Early apoptosis was defined as annexin V-positive/PI-negative and late apoptosis as annexin V/PI-double positive.

Transwell migration and invasion assays

Transwell migration and invasion assays were conducted in 24-well modified Boyden chambers (Transwell chambers; BD Transduction, Franklin Lakes, NJ). The upper surface of 6.4-mm-diameter filters with 8-μm pores was precoated with Matrigel (BD Transduction, Franklin Lakes, NJ) for the invasion assay or without Matrigel for the migration assay. HGC27 and

MKN45 cells (2×10^4 and 5×10^5 cells per well, respectively) and the activated CD8+ T cells at a ratio of 8:1, 0.5:1, and PBS as a control were transferred into the upper chamber. Following incubation for 22 h, all CD8+ T cells were collected and confirmed not to have permeated the filters. Then, the migrated or invasive cells on the lower surface of the filters were fixed and stained with Diff-Quik stain (Sysmex, Kobe, Japan). Stained cell nuclei were counted directly on filters in triplicate. We assessed the ability of the cells to move through extracellular matrices by calculating the ratio of the percentage of cells that invaded through the Matrigel-coated filters relative to the cells that migrated through the uncoated filters of test cells to that in the control cells.

Enzyme-linked immunosorbent assay

HGC27 and MKN45 cells, as target cells, were seeded into 6-well plates. Activated CD8+ T cells, as effector cells, were co-cultured with the cancer cells at ratios of 8:1, 0.5:1, and with PBS as a control. After co-culturing for 12 h, the supernatants from the co-culture were collected from the 6-well plates. Enzyme-linked immunosorbent assay (ELISA) was performed to measure the concentration of granzyme B using the human granzyme B sandwich ELISA Kit (Proteintech, IL), according to the manufacturer's protocol. Briefly, 100 µL of each standard granzyme B solution and co-culture supernatants were added to each well of an antibody-coated 96-well microplate and incubated for 2 h at 37°C. After incubation, the plate was washed four times with wash buffer, and residual buffer was removed. Next, 100 µL of anti-human granzyme B detection antibody solution was added to each well and incubated for 1 h at 37°C. The plate was washed again as described above. Then, 100 µL of streptavidin-horseradish peroxidase solution was added to each well and incubated for 40 min at 37°C. The plate was washed as before. Protected from light, 100 µL of tetramethylbenzidine (TMB) substrate solution was added to each well and incubated for 20 min at 37°C. Afterward, 100 µL of stop solution was added to each well in the same order as the TMB substrate solution. Immediately, absorbance values were measured at a wavelength of 450 nm using the Multiskan Fc with SkanIt software 3.1. Based on the absorbance of each standard granzyme B, a four-parameter logistic curve was generated, and the concentration of granzyme B in the co-culture supernatants was measured.

Statistical analysis

The chi-square test and Fisher's exact probability test were performed for categorical variables to compare the clinicopathological characteristics between groups. A multivariate analysis was performed using a logistic regression model. Overall and recurrence-free survival were estimated using the Kaplan-Meier method, and the log-rank test was used to assess differences between TILs. The Mann-Whitney U-test was used to assess the validity of the semi-quantitative evaluation. For *in vitro* analyses, analysis of variance followed by a post hoc Bonferroni test was used for the statistical analysis. A *P*-value of less than 0.05 was considered significant. Statistical analyses were performed using JMP Pro version 17.1.0.

Results

Characteristics of patients with advanced GC

Seventy-six of the 103 patients were male (73.8%), and the median age was 67 years. Median tumor size was 56 mm, and the number of patients with undifferentiated histological type was 54 (52.4%). The numbers of patients with venous invasion and lymphatic invasion were 58 (56.3%) and 71 (68.9%), respectively. The pathological diagnosis of tumor depth categories consisted of pT2 (n = 25, 24.3%), pT3 (n = 48, 46.6%) and pT4 (n = 30, 29.1%). The pathological lymph node metastasis categories consisted of pN0 (n = 49, 47.6%), pN1 (n = 17, 16.5%), pN2 (n = 16, 15.5%) and pN3 (n = 21, 20.4%) (**Table 1**).

Distribution of patients with each score of TIL_{IM} and TIL_{CT}

The distribution of the numbers of patients with TIL_{IM} and TIL_{CT} scores of 0 to 3+ is shown in **Figure 3**. None of the 103 patients showed no TILs in both the IM and CT. There were 3 patients each with a score of 0 in the IM only or the CT only, and 97 of 103 patients had TILs with a score of 1+ or higher in either the IM or the CT. Five of the six patients with a score of 3+ in the CT also had a score of 3+ in the IM.

Table 1. Clinicopathological characteristics of the study participants

Variable	Number (n = 103)
Sex	
Female	27 (26.2%)
Male	76 (73.8%)
Median age[a] (range)	67 (29-87)
BMI[b] (range)	21.7 (14.7-31.2)
Tumor location[c]	
U	29 (28.1%)
M	52 (50.5%)
L	22 (21.4%)
Median tumor size[d] (range)	56 (17-255)
Histological type	
Differentiated	49 (47.6%)
Undifferentiated	54 (52.4%)
Venous invasion	
Negative	45 (43.7%)
Positive	58 (56.3%)
Lymphatic invasion	
Negative	32 (31.1%)
Positive	71 (68.9%)
pT category[e]	
pT2	25 (24.3%)
pT3	48 (46.6%)
pT4	30 (29.1%)
pN category[e]	
pN0	49 (47.6%)
pN1	17 (16.5%)
pN2	16 (15.5%)
pN3	21 (20.4%)
pStage[e]	
I	17 (16.5%)
II	48 (46.6%)
III	38 (36.9%)

[a]Age in years; [b]Body mass index, kg/m^2; [c]U, upper third of the stomach; M, middle third of the stomach; L, lower third of the stomach; [d]mm; [e]The 8th edition of the International Union Against Cancer (UICC) TNM classification for gastric cancer.

The low and high TILs groups were color-coded white and grey, respectively.

Overall and recurrence-free survival of patients with advanced GC according to TILs score

First, we investigated the prognostic impact of CD8+ TILs infiltrating advanced GC. Survival curves based on TIL_{IM} and TIL_{CT} scores are shown in **Figure 4A** and **4B**. We confirmed that the greater the infiltration by both TIL_{IM} and TIL_{CT}, the better the prognosis in patients with advanced GC. In contrast, TIL_N showed no trend that could be used to stratify prognoses in a test-scale group of patients with advanced GC (**Figure 4C**). Therefore, to evaluate the potential of TILs as a prognostic marker, patients with advanced GC were divided into two groups based on TIL_{IM} and TIL_{CT}: a low TILs group and a high TILs group. The low TILs group had a significantly poorer prognosis in terms of recurrence-free survival compared with the high TILs group, as shown in **Figure 5**.

Clinicopathological factors associated with TIL_{IM} and TIL_{CT}

We next investigated clinicopathological factors associated with CD8+ TILs based on the sites of their infiltration in advanced GC. First, we investigated the association between clinicopathological factors and TIL_{IM} in advanced GC. Our univariate analysis showed that patients with low TIL_{IM} were more likely to be female, younger, and have undifferentiated histological types and deeper tumor invasion compared to those with high TIL_{IM}. In our multivariate analysis using a logistic regression model, deeper tumor invasion was identified as an independent risk factor for patients with low TIL_{IM} (**Table 2**). Second, we investigated the association between clinicopathological factors and TIL_{CT} in advanced GC. Our univariate analysis showed that patients with low TIL_{CT} had significantly more positive lymph node metastasis compared to those with high TIL_{CT}. In our multivariate analysis using a logistic regression model, positive lymph node metastasis was found to be an independent risk-factor for patients with low TIL_{CT} (**Table 3**).

Association between clinicopathological factors and TILs score

Finally, we investigated clinicopathological factors associated with the TILs score in advanced GC. Our univariate analysis showed that patients in the low TILs group had significantly larger tumor diameter, deeper tumor invasion, and more positive lymph node metastasis than those in the high TILs group. In our multivariate analysis using a logistic regression model, deeper tumor invasion was an independent risk factor for patients in the low TILs group (**Table 4**).

Distribution numbers of each score of TILs at the invasive margin (TIL_{IM}) and the center of the tumor (TIL_{CT}).

TIL_{CT} \ TIL_{IM}	0	1+	2+	3+
0	0	2	1	0
1+	3	32	13	1
2+	0	18	22	5
3+	0	0	1	5

Low TILs group
High TILs group

Figure 3. Distribution of the numbers of patients with each score of TILs in the invasive margin (TIL_{IM}) and the center of the tumor (TIL_{CT}) of gastric cancer (GC). The low and the high TILs groups are color-coded white and grey, respectively.

Association between quantitative and semi-quantitative evaluation of TILs

A quantitative evaluation method was used to verify the validity of the semi-quantitative evaluation. Patients with the low semi-quantitative TIL_{IM} and TIL_{CT} had significantly lower quantitative TIL_{IM} and TIL_{CT} compared to those with the high semi-quantitative TIL_{IM} and TIL_{CT} (**Figure 6A** and **6B**). Furthermore, the low semi-quantitative TILs group had significantly lower quantitative TILs than the high semi-quantitative TILs group (**Figure 6C**). However, in patients classified in the high semi-quantitative TIL_{IM}, TIL_{CT}, and TILs groups, some patients had the low quantitative TIL_{IM}, TIL_{CT}, and TILs, respectively (**Figure 6A-C**).

Overall and recurrence-free survival according to quantitative TILs in the high semi-quantitative TILs group, and clinicopathological factors associated with low quantitative TILs in the high semi-quantitative TILs group

Patients with low quantitative TILs in the high semi-quantitative TILs group might be misclassified as having lower malignancy, which could have a critical impact on the treatment selection. Therefore, to investigate the prognosis of patients with differing results between semi-quantitative and quantitative evaluations of TILs, we analyzed survival curves based on quantitative TILs in the high semi-quantitative TILs group in advanced GC. We confirmed that patients with low quantitative TILs tended to have poorer survival than those with high quantitative TILs (**Figure 6D**). Next, to investigate why patients classified in the high semi-quantitative TILs group had low quantitative TILs, we investigated clinicopathological factors associated with low quantitative TILs in the high semi-quantitative TILs group in advanced GC. Our univariate analysis showed that patients with low quantitative TILs in the high semi-quantitative TILs group had significantly deeper tumor invasion than those with high quantitative TILs in the same group (**Table 5**).

Suppression of cell proliferation by CD8+ T cells in GC cell lines

The high TILs group showed better oncologic prognosis than the low TILs group, so we tested the oncologic effects of the degree of CD8+ TILs infiltration *in vitro*. We performed a cell proliferation assay using two different effector cell:target cell (ET) ratios to investigate whether a high density of CD8+ T cells could suppress the proliferation of GC cells. In both HGC27 (derived from lymphatic metastasis adenocarcinoma) and MKN45 (derived from poorly differentiated adenocarcinoma) cells, the target cell viability with an ET ratio of 8:1 (high TILs) was compared with an ET ratio of 0.5:1 (low TILs) and negative controls. The proliferation of both cell lines with an ET ratio of 8:1 was signifi-

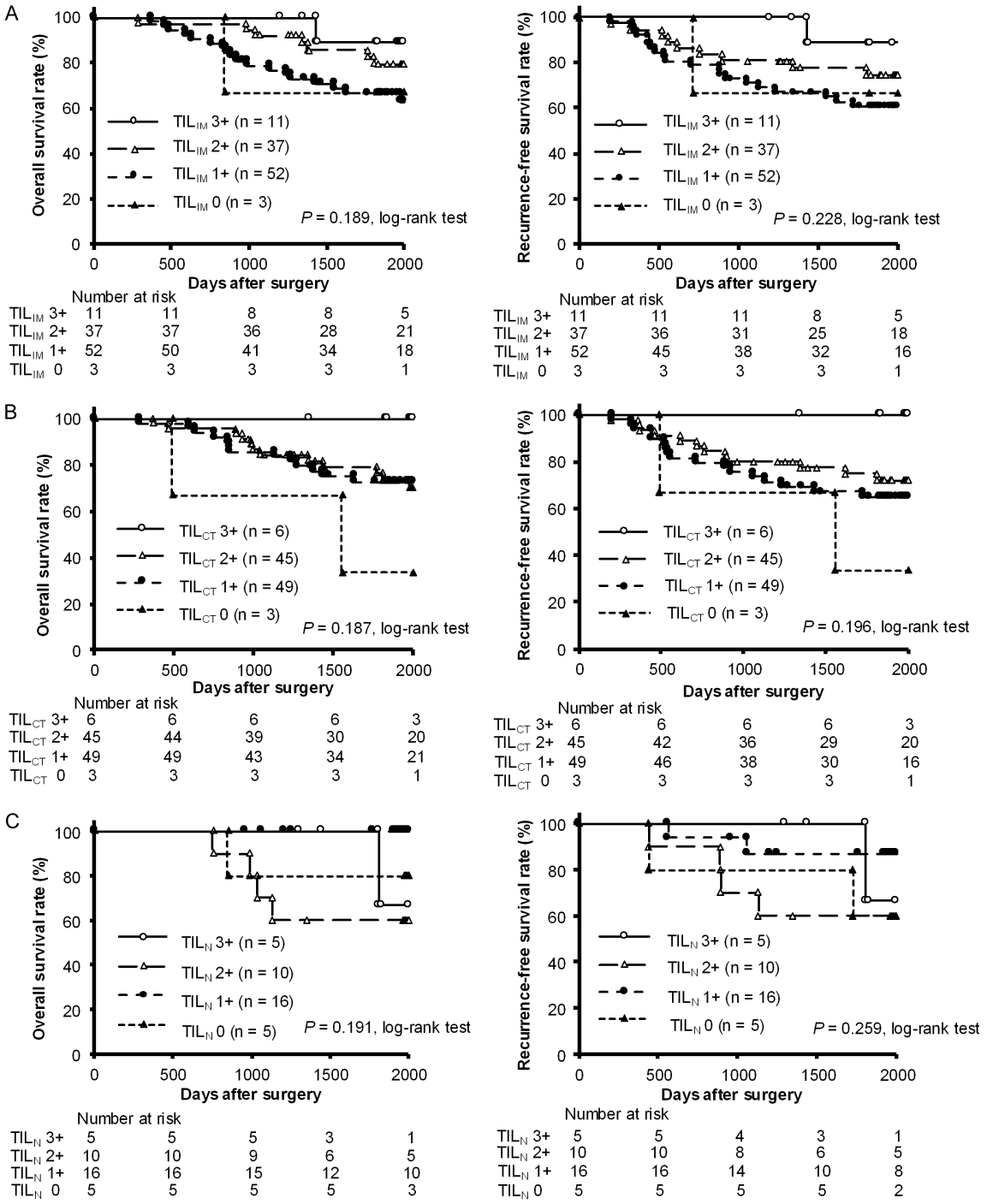

Figure 4. Analysis of overall survival and recurrence-free survival rates of patients with GC based on TILs in the invasive margin (TIL_{IM}) (A), the center of the tumor (TIL_{CT}) (B), and the tumor nests (TIL_{N}) (C). The log-rank test was used for the statistical analysis. $P < 0.05$ was considered statistically significant.

cantly lower than with an ET ratio of 0.5:1 and negative controls. However, there was no difference in the proliferation of either cell line with an ET ratio of 0.5:1 and negative controls (**Figure 7A**).

Induced apoptosis by CD8+ T cells in GC cell lines

We next performed an apoptosis assay to investigate the reasons for the suppression of

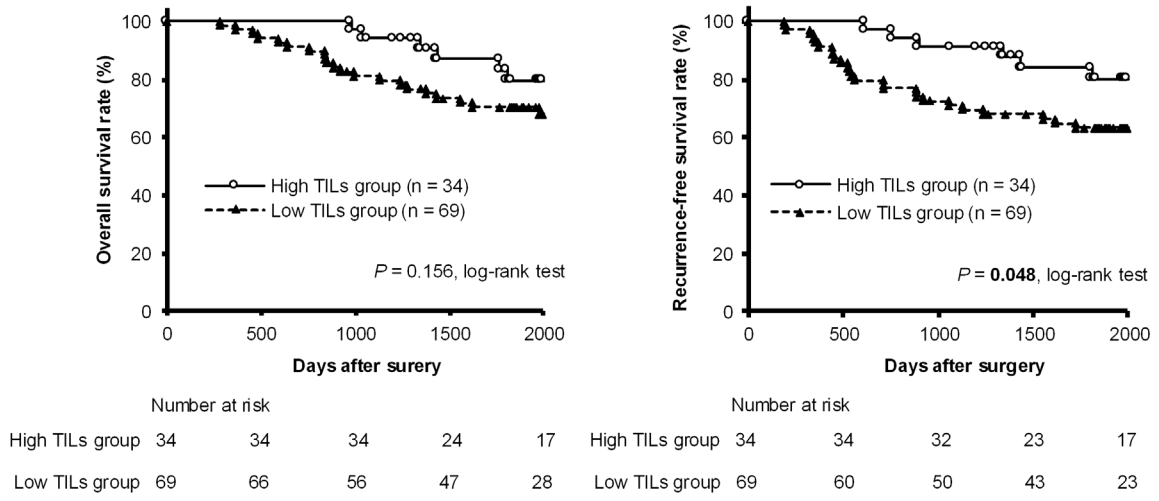

Figure 5. Analysis of overall survival and recurrence-free survival rate of patients with GC in the low or high TILs groups. The log-rank test was used for the statistical analysis. $P < 0.05$ was considered statistically significant.

cell proliferation by a high density of CD8+ T cells. Fluorescence-activated cell sorting analysis demonstrated that the number of cells in early apoptosis and late apoptosis was significantly higher when co-cultured with an ET ratio of 8:1 compared with an ET ratio of 0.5:1 and negative controls (PBS). However, there was no difference in the number of cells in early and late apoptosis between either cell line with an ET ratio of 0.5:1 and negative controls (**Figure 7B**).

Suppression of cell migration and invasion by CD8+ T cells in GC cell lines

To examine the effect of CD8+ T cells on the migratory and invasive capacity of cancer cells *in vitro*, transwell migration and invasion assays were performed. We examined the ability of HGC27 and MKN45 cells co-cultured with CD8+ T cells to move through pores under different ET ratios. An uncoated membrane was used for the migration assays, whereas a Matrigel-coated membrane was used for the invasion assays. The numbers of HGC27 and MKN45 cells co-cultured with CD8+ T cells with an ET ratio of 8:1 that migrated into the lower chamber were significantly lower than those co-cultured with an ET ratio of 0.5:1 and negative controls. However, there was no difference in the migratory and invasive capacity of either cell line between those with an ET ratio of 0.5:1 and negative controls (**Figure 7C**). This result suggests that CD8+ T cells not only induce apoptosis of cancer cells but also might influence their migration and invasion capacity.

Granzyme B secreted by CD8+ T cells

To clarify the molecular dynamics behind the apoptosis of cancer cells and the suppression of cancer cell migration and invasion in co-culture with CD8+ T cells, we measured the change in granzyme B concentration in the culture medium. ELISA demonstrated that the concentration of granzyme B was significantly higher when co-cultured with an ET ratio of 8:1 compared to an ET ratio of 0.5:1 and negative controls (PBS). However, there was no difference in the concentration of granzyme B between either cell line with an ET ratio of 0.5:1 and negative controls (**Figure 7D**).

Discussion

In this study, we validated a method for evaluating TILs based on their infiltration site in GC and investigated the potential of CD8+ TILs as a prognostic marker in advanced GC. We clarified the clinicopathological characteristics of TILs according to their infiltration site in GC. Furthermore, we demonstrated the usefulness and limitations of semi-quantitative scoring methods for CD8+ TILs in GC. Additionally, we also confirmed the tumor suppressive effect of CD8+ T cells in a concentration-dependent manner in GC cell lines *in vitro.*

A specific recommended evaluation method for TILs has been determined for various cancers, including breast cancer, melanoma, colorectal cancer, non-small cell lung cancer, ovarian cancer, head and neck squamous cell cancer and

Table 2. Univariate and multivariate analyses of factors influencing TILs scores in the invasive margin, using a logistic regression model

	n	TIL_{IM}[a]				Univariate[b]	Multivariate[c]		
		Low		High		*P*-value	OR[d]	95% CI[e]	*P*-value
Total	103	55		48					
Sex									
Female	27	19	-35%	8	-17%				
Male	76	36	-65%	40	-83%	**0.04**			
Age (years)									
< 75	84	49	-89%	35	-73%				
≥ 75	19	6	-11%	13	-27%	**0.035**			
BMI[f] (kg/m^2)									
≥ 18.5	88	46	-84%	42	-88%				
< 18.5	15	9	-16%	6	-12%	0.579			
Tumor location[g]									
U	36	16	-29%	20	-42%				
M, L	67	39	-71%	28	-58%	0.182			
Tumor size (mm)									
< 50	41	18	-33%	23	-48%				
≥ 50	62	37	-67%	25	-52%	0.116			
Histological type									
Differentiated	49	21	-38%	28	-58%				
Undifferentiated	54	34	-62%	20	-42%	**0.041**			
Venous invasion									
V0-2	81	46	-84%	35	-73%				
V3	22	9	-16%	13	-27%	0.185			
Lymphatic invasion									
Ly0-2	57	30	-55%	27	-56%				
Ly3	46	25	-45%	21	-44%	0.862			
pT category[h]									
pT2-3	73	32	-58%	41	-85%				
pT4	30	23	-42%	7	-15%	**0.002**	4.13	1.51-11.32	**0.004**
pN category[h]									
pN0	49	23	-42%	26	-54%				
pN1-3	54	32	-58%	22	-46%	0.211			

[a]TIL_{IM}, tumor-infiltrating lymphocytes in the invasive margin; [b]The chi-square test and Fisher's exact probability test were performed; [c]Multivariate analysis was performed using a logistic regression model; [d]OR, odds ratio; [e]CI, confidence interval; [f]BMI, body mass index; [g]U, upper third of the stomach; M, middle third of the stomach; L, lower third of the stomach; [h]The 8th edition of the International Union Against Cancer (UICC) TNM classification for gastric cancer. Values in bold represent $P < 0.05$.

genitourinary cancer [18]. In particular, in the field of breast cancer, evaluation methods for TILs are internationally established and their importance is widely known [3, 22, 23]. However, no evaluation methods for TILs in GC have yet been established, and the importance of TILs in GC remains unclear. In fact, initial evidence suggests that only stromal TILs should be evaluated in GC due to the lack of prognostic significance of intra-tumoral TILs; however, this finding requires further validation [18]. The prognostic significance of intra-tumoral TILs has been clarified in several cancers. Methods for evaluating TILs in melanoma typically focus solely on intra-tumoral TILs, which are associated with favorable outcomes in patients with melanoma [24, 25]. In ovarian cancer, both stromal TILs and intra-tumoral TILs are relevant for prognosis and therefore both are evaluated [26, 27]. We also retrospectively analyzed intra-tumoral TILs in this study. However, TIL_N showed no trend that could be used to stratify progno-

Table 3. Univariate and multivariate analyses of factors influencing TILs scores in the center of the tumor, using a logistic regression model

	n	TIL_{CT}[a]				Univariate[b]	Multivariate[c]		
		Low		High		*P*-value	OR[d]	95% CI[e]	*P*-value
Total	103	52		51					
Sex									
Female	27	15	-29%	12	-24%				
Male	76	37	-71%	39	-76%	0.54			
Age (years)									
< 75	84	43	-83%	41	-80%				
≥ 75	19	9	-17%	10	-20%	0.764			
BMI[f] (kg/m^2)									
≥ 18.5	88	43	-83%	45	-88%				
< 18.5	15	9	-17%	6	-12%	0.425			
Tumor location[g]									
U	36	18	-35%	18	-35%				
M, L	67	34	-65%	33	-65%	0.942			
Tumor size (mm)									
< 50	41	19	-37%	22	-43%				
≥ 50	62	33	-63%	29	-57%	0.494			
Histological type									
Differentiated	49	29	-56%	20	-39%				
Undifferentiated	54	23	-44%	31	-61%	0.093			
Venous invasion									
V0-2	81	39	-75%	42	-82%				
V3	22	13	-25%	9	-18%	0.363			
Lymphatic invasion									
Ly0-2	57	26	-50%	31	-61%				
Ly3	46	26	-50%	20	-39%	0.271			
pT category[h]									
pT2-3	73	33	-63%	40	-78%				
pT4	30	19	-37%	11	-22%	0.095			
pN category[h]									
pN0	49	19	-37%	30	-59%				
pN1-3	54	33	-63%	21	-41%	**0.024**	2.48	1.12-5.49	**0.023**

[a]TIL_{CT}, tumor-infiltrating lymphocytes in the center of the tumor; [b]The chi-square test and Fisher's exact probability test were performed; [c]Multivariate analysis was performed using a logistic regression model; [d]OR, odds ratio; [e]CI, confidence interval; [f]BMI, body mass index; [g]U, upper third of the stomach; M, middle third of the stomach; L, lower third of the stomach; [h]The 8th edition of the International Union Against Cancer (UICC) TNM classification for gastric cancer. Values in bold represent $P < 0.05$.

ses in a test-scale number of patients with advanced GC. Therefore, in this study, we investigated whether the sum of the scores of stromal TILs in the IM and CT, without using the TIL_N score, was a suitable index for the prognostic stratification of patients with GC.

There are some reasons for why the significance of TILs in GC has yet to be determined. First, there are morphological differences between GC and other solid tumors such as breast cancer. With breast cancer, the percentage of stromal TILs inside a tumor can be evaluated by hematoxylin and eosin (H&E) staining [22, 23]. However, in GC, which is a cancer derived from the gastrointestinal epithelium, evaluating the percentage of stromal TILs inside a tumor alone is insufficient as there is another important prognostic factor to consider, i.e., the depth of tumor invasion. For this

Table 4. Univariate and multivariate analyses of factors influencing TILs scores, using a logistic regression model

	n	TILs[a] score				Univariate[b]	Multivariate[c]		
		Low TILs group		High TILs group		*P*-value	OR[d]	95% CI[e]	*P*-value
Total	103	69		34					
Sex									
Female	27	22	-32%	5	-15%				
Male	76	47	-68%	29	-85%	0.062			
Age (years)									
< 75	84	59	-86%	25	-74%				
≥ 75	19	10	-14%	9	-26%	0.141			
BMI[f] (kg/m^2)									
≥ 18.5	88	57	-83%	31	-91%				
< 18.5	15	12	-17%	3	-9%	0.229			
Tumor location[g]									
U	36	23	-33%	13	-38%				
M, L	67	46	-67%	21	-62%	0.625			
Tumor size (mm)									
< 50	41	22	-32%	19	-56%				
≥ 50	62	47	-68%	15	-44%	**0.019**			
Histological type									
Differentiated	49	31	-45%	18	-53%				
Undifferentiated	54	38	-55%	16	-47%	0.444			
Venous invasion									
V0-2	81	52	-75%	29	-85%				
V3	22	17	-25%	5	-15%	0.248			
Lymphatic invasion									
Ly0-2	57	36	-52%	21	-62%				
Ly3	46	33	-48%	13	-38%	0.357			
pT category[h]									
pT2-3	73	42	-61%	31	-91%				
pT4	30	27	-39%	3	-9%	**0.001**	5.25	1.57-24.11	**0.006**
pN category[h]									
pN0	49	27	-39%	22	-65%				
pN1-3	54	42	-61%	12	-35%	**0.015**			

[a]TILs, tumor-infiltrating lymphocytes; [b]The chi-square test and Fisher's exact probability test were performed; [c]Multivariate analysis was performed using a logistic regression model; [d]OR, odds ratio; [e]CI, confidence interval; [f]BMI, body mass index; [g]U, upper third of the stomach; M, middle third of the stomach; L, lower third of the stomach; [h]The 8th edition of the International Union Against Cancer (UICC) TNM classification for gastric cancer. Values in bold represent $P < 0.05$.

reason, the evaluation of TILs in GC is more complicated than in other solid tumors such as breast cancer. Second, previous reports have evaluated different subtypes of TILs in GC, and the evaluation methods used were not consistent. There have been some reports of methods where TILs in GC are simply counted per HPF [28-30]. No specific objects to be evaluated were determined, such as Foxp3+, CD3+, or CD8+ T cells by immunohistochemistry or all lymphocytes by HE staining [28-31]. Recently, it was reported that scoring methods for TILs in different parts of a tumor may be useful for GC prognosis [17, 32]. Considering the morphological characteristics of GC, we evaluated TILs not only in the CT but also the IM. Additionally, we evaluated CD8+ TILs, because GC with TILs of this subtype has been reported to have a more favorable prognosis compared with GC with other TIL subtypes [28, 33]. Few previous studies have scored CD8+ TILs in the IM and CT in GC. Therefore, the findings of the present study

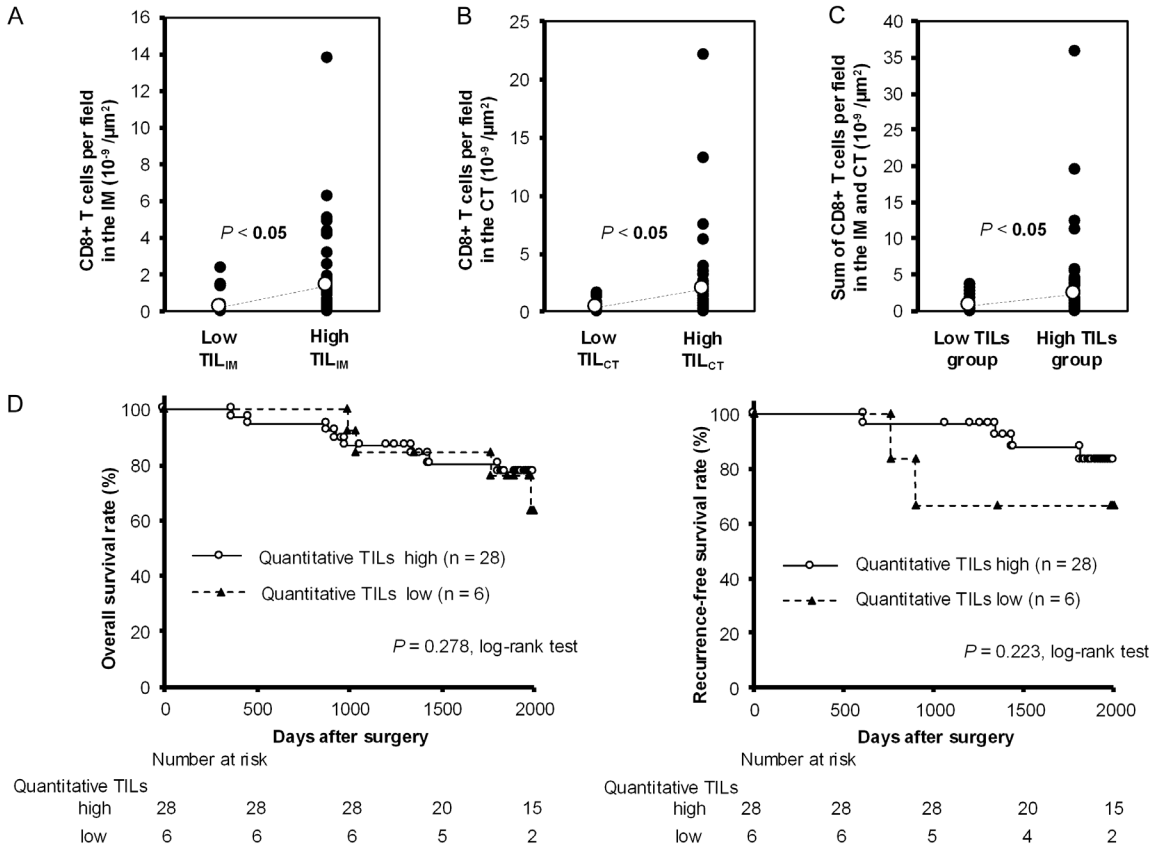

Figure 6. (A-C) A quantitative evaluation method was used to verify the validity of the semi-quantitative evaluation. CD8+ T cells per field in the IM (10^{-9}/μm^2) of GC were quantitatively evaluated (A). CD8+ T cells per field in the CT (10^{-9}/μm^2) of GC were quantitatively evaluated (B). The sum of CD8+ T cells per field in the IM and CT (10^{-9}/μm^2) of GC were quantitatively evaluated (C). The Mann-Whitney U-test was used for the statistical analysis. $P < 0.05$ was considered statistically significant. (D) Analysis of overall survival and recurrence-free survival rates in patients with GC based on quantitative TILs (the sum of the quantitative TILs in the IM and the CT) in the high semi-quantitative TILs group. The log-rank test was used for the statistical analysis. A *P*-value of < 0.05 was considered statistically significant.

have clinical relevance for GC treatment and care. In this study, however, other immune cells were not evaluated. CD8+ T cells are prone to becoming dysfunctional and unresponsive to cancer cells over the course of tumorigenesis. However, tumor-specific CD4+ T cells prevent and reverse CD8+ T cell dysfunction [34, 35]. On the other hand, the infiltration of Treg cells represents immune suppression in tumors. Whereas dendritic cells are involved in intratumoral CD8+ T cell differentiation and expansion and promote cancer immune control, Treg cells located near dendritic cells in tumors suppress tumor antigen presentation and impede the antitumor CD8+ T cell response [36, 37]. Tumor-associated macrophages constitute the majority of immune components infiltrating tumors, and they are further categorized into anti-tumor M1 and pro-tumor M2 subtypes [38]. There is a bidirectional interaction between tumor cells and tumor-infiltrating cells that determines macrophage polarization and, ultimately, tumor progression or regression [39]. In this study, these synergistic or antagonistic immune interactions were not investigated, and caution is required in interpreting the results.

Furthermore, we used a semi-quantitative method to evaluate CD8+ TILs because quantitative methods in previous reports using H&E staining and calculating percentages are complex and lack versatility [17, 32]. When evaluating TILs by H&E staining, other infiltrating immune cells, including neutrophils, and any other cells must be excluded, which requires a well-trained and experienced pathologist. Previous reports have used a method of evalu-

Table 5. Univariate analysis of factors influencing quantitative TILs in the high TILs group

	Quantitative TILs[a] in IM[b] and CT[c] in high TILs group				Univariate[d]
	Low		High		*P*-value
Total	6		28		
Sex					
Female	0	0%	5	-18%	
Male	6	-100%	23	-82%	0.146
Age (years)					
< 75	5	-83%	20	-71%	
≥ 75	1	-17%	8	-29%	0.533
BMI[e] (kg/m^2)					
≥ 18.5	6	-100%	25	-89%	
< 18.5	0	0%	3	-11%	0.268
Tumor location[f]					
U	3	-50%	10	-36%	
M, L	3	-50%	18	-64%	0.518
Tumor size (mm)					
< 50	3	-50%	16	-57%	
≥ 50	3	-50%	12	-43%	0.75
Histological type					
Differentiated	2	-33%	16	-57%	
Undifferentiated	4	-67%	12	-43%	0.287
Venous invasion					
V0-2	6	-100%	23	-82%	
V3	0	0%	5	-18%	0.146
Lymphatic invasion					
Ly0-2	3	-50%	18	-64%	
Ly3	3	-50%	10	-36%	0.518
pT category[g]					
pT2-3	4	-67%	27	-96%	
pT4	2	-33%	1	-4%	**0.045**
pN category[g]					
pN0	3	-50%	19	-68%	
pN1-3	3	-50%	9	-32%	0.414

[a]TILs, tumor-infiltrating lymphocytes; [b]IM, invasive margin; [c]CT, center of the tumor; [d]The chi-square test and Fisher's exact probability test were performed; [e]BMI, body mass index; [f]U, upper third of the stomach; M, middle third of the stomach; L, lower third of the stomach; [g]The 8th edition of the International Union Against Cancer (UICC) TNM classification for gastric cancer. Values in bold represent $P < 0.05$.

ation by H&E staining based on a value calculated by multiplying the semi-quantitative evaluation value by the qualitative evaluation value, but this approach is very complicated [17, 32]. Our method addresses this issue, because it only involves a semi-quantitative evaluation method for GC. However, it should be noted that whereas most patients in the low TILs group classified by the semi-quantitative scoring method also had low quantitative TILs, some patients in the high semi-quantitative TILs group had low quantitative TILs. It is important to recognize that these patients with low quantitative TILs in the high semi-quantitative TILs group tended to have poorer survival than those with high quantitative TILs in the high semi-quantitative TILs group. Additionally, the characteristic of these patients with low quantitative TILs in the high semi-quantitative TILs group was that their tumors exhibited deep invasion. It was suggested that even expert pathologists find it difficult to evaluate TILs in clinical GC samples with deeper tumor invasion. This challenge is likely due to the difficulty in distinguishing the border of the IM when the serosa is invaded by cancer.

It has been reported that TILs are associated with microsatellite instability-high, chronic inflammation due to *Helicobacter pylori* and Epstein-Barr virus (EBV) infections, and tumor mutation burden in patients with GC [40-46]. In particular, it has been reported that stratifying GC patients by molecular subtypes identifies subtype-specific TIL dynamics. EBV-positive GCs are associated with high infiltration of CD3+ T cells and CD8+ T cells in GC patients [41, 45, 46]. Some studies have shown that MSI-high is associated with high levels of CD8+ T cells and Treg cells, whereas other reports have shown that it is not associated with CD3+ TILs in GC patients [42, 46]. Moreover, TILs in GC are associated with favorable oncological characteristics, such as a shallow depth of tumor invasion and limited incidence of lymph node metastasis [32, 47, 48]. Interestingly, our analysis by TIL site showed that patients with low TIL_{IM} were significantly more likely to be female, younger, and have undifferentiated histological types and deeper tumor invasion.

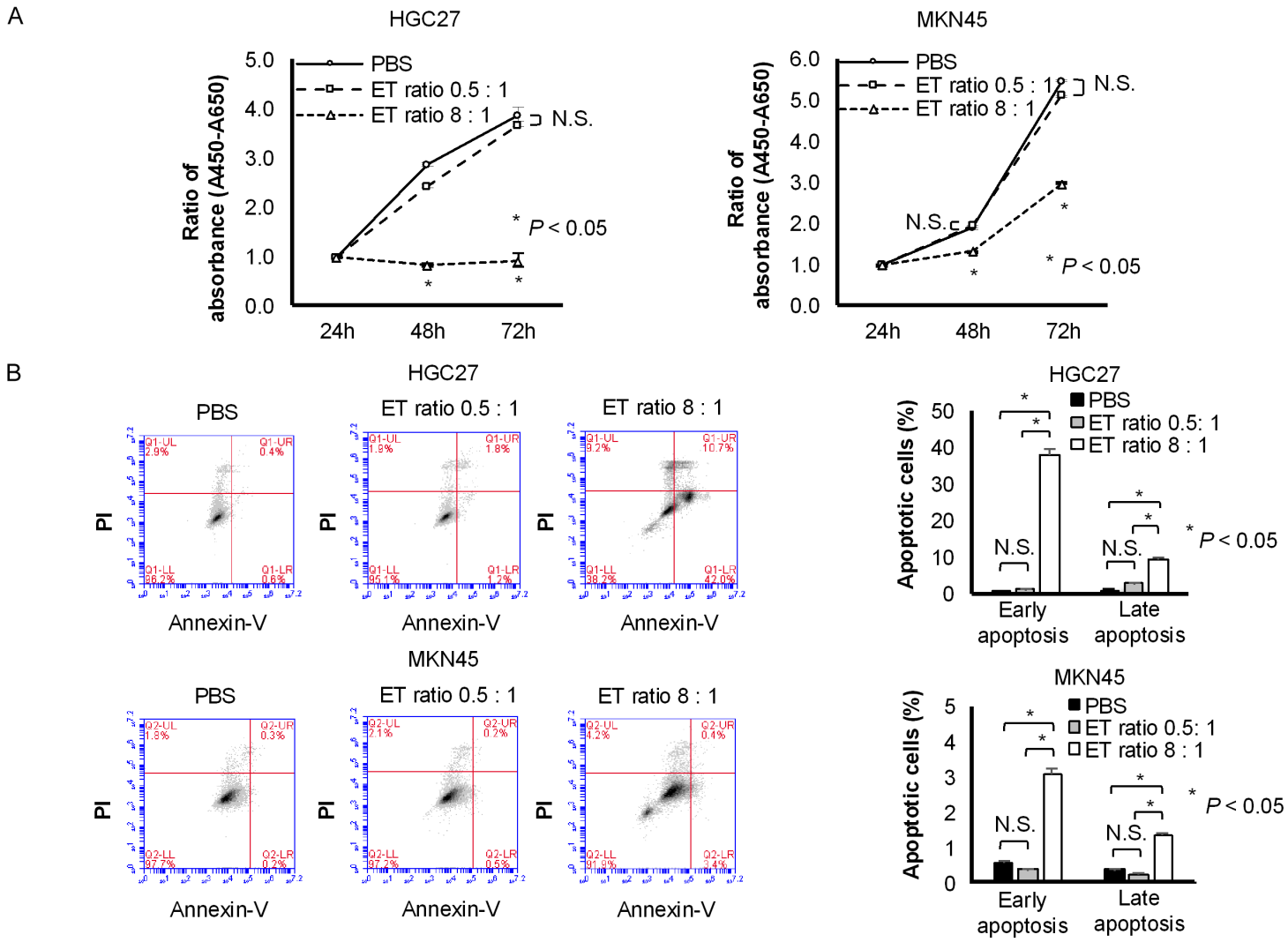
A
HGC27
MKN45
PBS
ET ratio 0.5 : 1
ET ratio 8 : 1
Ratio of absorbance (A450-A650)
N.S.
* P < 0.05
24h
48h
72h
B
HGC27
PBS
ET ratio 0.5 : 1
ET ratio 8 : 1
PI
Annexin-V
MKN45
Apoptotic cells (%)
Early apoptosis
Late apoptosis

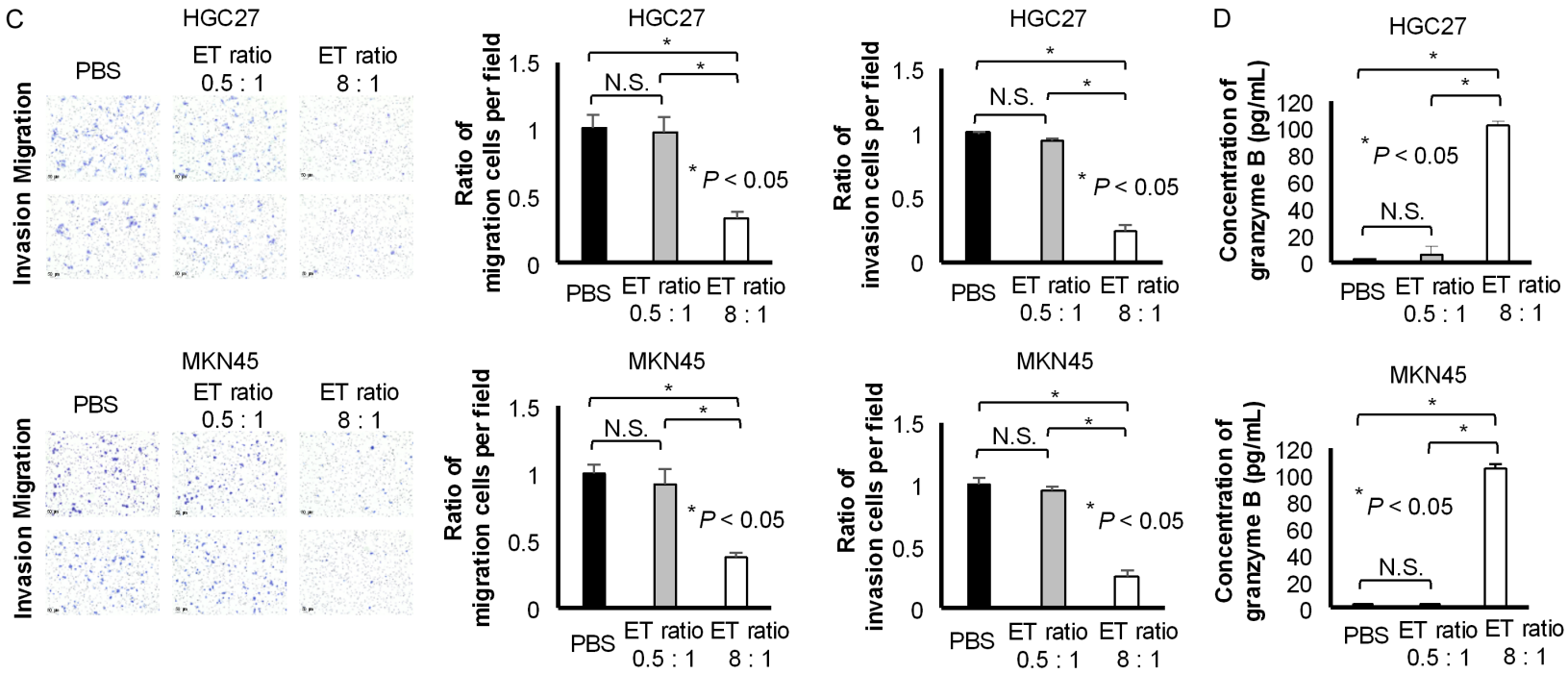

Figure 7. A. Effect of CD8+ T cells on cell proliferation at the indicated times. *$P < 0.05$, vs. the phosphate-buffered saline (PBS) or effector cell:target cell (ET) ratio 0.5:1. B. Representative results of the apoptosis assay in GC cells at 72 h after co-culture with CD8+ T cells. *$P < 0.05$, vs. the PBS or ET ratio 0.5:1. C. Migration and invasion of cells 22 h after co-culture of CD8+ T cells with HGC27 and MKN45 cells. *$P < 0.05$, vs. the PBS or ET ratio 0.5:1. D. Concentration of granzyme B in the co-culture supernatants 12 h after co-culturing CD8+ T cells with HGC27 and MKN45 cells. *$P < 0.05$, vs. the PBS or ET ratio 0.5:1. These results are the means + standard error (bars) for experiments conducted in duplicate or triplicate. Analysis of variance followed by a post hoc test of Bonferroni was used for the statistical analysis.

These clinicopathological characteristics are commonly observed in scirrhous GC, which is associated with an extremely poor prognosis [49-51]. This finding suggests that TIL_{IM} may be closely related to scirrhous GC, and investigating TIL_{IM} in scirrhous GC may provide valuable insights. Additionally, deeper tumor invasion was an independent risk factor for low TIL_{IM}, whereas lymph node metastasis was an independent risk factor for low TIL_{CT}. There have been no previous reports showing that differences in the locations of TILs, such as TIL_{IM} and TIL_{CT}, are linked with different oncological characteristics in many cancers, including GC. It has been suggested that in GC, TILs can enhance host antitumor immunity and prevent tumor cells from invading and metastasizing [47, 52]. Therefore, we might interpret the present results to mean that TIL_{IM} and TIL_{CT}, limit the depth of a tumor and lymph node metastasis, respectively, by enhancing antitumor immunity. This suggests that TILs in different regions of a tumor might be important factors involved in the mechanism of suppressing tumor invasion and metastasis. In the future, it will be worth further investigating TILs by site within the tumor in the tumor microenvironment.

In recent years, there has been increasing awareness of the role played by T cells in the tumor microenvironment, and several *in vitro* experiments have been conducted involving co-culture systems of T cells and cancer cells [53-55]. As we found that CD8+ TILs were related to the depth of tumor invasion and resulted in favorable recurrence-free survival in patients with GC, we next conducted experiments to investigate the tumor microenvironment using a co-culture system of CD8+ T cells and cancer cells. We verified the tumor suppressive effects using various ET ratios to simplify the ratio of CD8+ T cells and cancer cells in the tumor microenvironment. We confirmed that tumor growth in GC cell lines was suppressed through the induction of apoptotic cells in a concentration-dependent manner by CD8+ T cells. This indicates that the concentration of CD8+ T cells is strongly involved in tumor suppression. Moreover, we confirmed that granzyme B was secreted by CD8+ T cells in a concentration-dependent manner during co-culture. In particular, this raises the interesting possibility that CD8+ T cells suppress tumor migration and invasion through the action of granzyme B. Granzyme B, which is secreted by T lymphocytes, has been reported to induce apoptosis in tumor cells in the presence of perforin, and it also plays a role in inhibiting the epithelial-mesenchymal transition (EMT) of tumors by cleaving extracellular matrix proteins and altering the structure of the extracellular matrix [56-58]. Our results may support these previous reports, suggesting that granzyme B secreted by CD8+ T cells suppresses tumor EMT.

There are several limitations to our study. First, it was a retrospective study, involving an analysis of a small number of patients with GC, from a single institute. Therefore, a prospective, observational study involving several large cohorts should be conducted to validate the impact of our semi-quantitative scoring method for CD8+ TILs in GC. Second, in this study, we used a mimic of activated CD8+ T cells after antigen presentation *in vivo* by activating CD8+ T cells with anti-CD3 and anti-CD28 antibodies. Therefore, it is important to note that the actual process of antigen presentation was omitted and the matching of human leukocyte antigen types was not clarified. Moreover, we only investigated TILs that comprised CD8+ T cells. However, the actual tumor microenvironment is extremely complex, and further detailed research into the tumor microenvironment is needed in the future. Finally, GC exhibits considerable intra-tumor heterogeneity, so the degree of infiltration of TILs might differ in different parts, so this issue should also be considered in any future evaluations of the role TILs play in GC.

We have proposed a novel semi-quantitative scoring method for TILs based on their infiltration site in GC, using immunostaining of CD8+ T cells. According to our simple and versatile semi-quantitative scoring method for CD8+ TILs, CD8+ TILs can be sensitive prognostic markers in GC, suppressing tumor progression. While the reliability of low TILs determined by the semi-quantitative scoring method is higher, we have demonstrated the limitations of evaluating TILs in clinical samples of GC with deeper tumor invasion, which remains challenging even for expert pathologists. This evaluation method represents a highly versatile biomarker for GC that could be widely used and contribute to improved prognoses in patients with GC.

Acknowledgements

We would like to express our sincere gratitude to all of the individuals who supported this research and offered their expertise and cooperation in the preparation of the manuscript.

Disclosure of conflict of interest

None.

Address correspondence to: Dr. Jun Kiuchi, Division of Digestive Surgery, Department of Surgery, Kyoto Prefectural University of Medicine, 465 Kajii-cho, Kawaramachi-Hirokoji, Kamigyo-ku, Kyoto 602-8566, Japan. Tel: +81-75-251-5527; Fax: +81-75-251-5522; E-mail: kiuchi@koto.kpu-m.ac.jp

References

[1] Siegel RL, Giaquinto AN and Jemal A. Cancer statistics, 2024. CA Cancer J Clin 2024; 74: 12-49.

[2] Etoh T, Ohyama T, Sakuramoto S, Tsuji T, Lee SW, Yoshida K, Koeda K, Hiki N, Kunisaki C, Tokunaga M, Otsubo D, Takagane A, Misawa K, Kinoshita T, Cho H, Doki Y, Nunobe S, Shiraishi N and Kitano S; Japanese Laparoscopic Surgery Study Group (JLSSG). Five-year survival outcomes of laparoscopy-assisted vs open distal gastrectomy for advanced gastric cancer: the JLSSG0901 randomized clinical trial. JAMA Surg 2023; 158: 445-454.

[3] Stanton SE and Disis ML. Clinical significance of tumor-infiltrating lymphocytes in breast cancer. J Immunother Cancer 2016; 4: 59.

[4] Badalamenti G, Fanale D, Incorvaia L, Barraco N, Listi A, Maragliano R, Vincenzi B, Calo V, Iovanna JL, Bazan V and Russo A. Role of tumor-infiltrating lymphocytes in patients with solid tumors: can a drop dig a stone? Cell Immunol 2019; 343: 103753.

[5] Williams CJM, Gray R, Hills RK, Shires M, Zhang L, Zhao Z, Gardner T, Sapanara N, Xu XM, Bai I, Yan D, Muranyi A, Dance S, Aghaei F, Hemmings G, Hale M, Kurkure U, Guetter C, Richman SD, Hutchins G, Seligmann JF, West NP, Singh S, Shanmugam K and Quirke P. Evaluation of CD3 and CD8 T-cell immunohistochemistry for prognostication and prediction of benefit from adjuvant chemotherapy in early-stage colorectal cancer within the QUASAR trial. J Clin Oncol 2024; 42: 3430-3442.

[6] DeNardo DG, Andreu P and Coussens LM. Interactions between lymphocytes and myeloid cells regulate pro- versus anti-tumor immunity. Cancer Metastasis Rev 2010; 29: 309-316.

[7] Mellman I, Chen DS, Powles T and Turley SJ. The cancer-immunity cycle: indication, genotype, and immunotype. Immunity 2023; 56: 2188-2205.

[8] Rieth J and Subramanian S. Mechanisms of intrinsic tumor resistance to immunotherapy. Int J Mol Sci 2018; 19: 1340.

[9] Japanese Gastric Cancer Association. Japanese Gastric Cancer Treatment Guidelines 2021 (6th edition). Gastric Cancer 2023; 26: 1-25.

[10] Japanese Gastric Cancer Association. Japanese classification of gastric carcinoma the 15th edition. 2017.

[11] Brierley JD, Gospodarowicz MK, Wittekind C, et al. TNM Classification of Malignant Tumours. 8th edition. 2016.

[12] Katikireddy KR and O'Sullivan F. Immunohistochemical and immunofluorescence procedures for protein analysis. Methods Mol Biol 2011; 784: 155-167.

[13] Tran DTP, Kuchimaru T, Pongsuchart M, Nguyen KT, Co Soriano JC, Kadonosono T and Kizaka-Kondoh S. ROR2 regulates the survival of murine osteosarcoma cells in lung capillaries. J Cancer Metastasis Treat 2020; 6: 1-11.

[14] Kaneshige A, Kaji T, Saito H, Higashimoto T, Nakamura A, Kurosawa T, Ikemoto-Uezumi M, Uezumi A and Fukada SI. Detection of muscle stem cell-derived myonuclei in murine overloaded muscles. STAR Protoc 2022; 3: 101307.

[15] Klintrup K, Makinen JM, Kauppila S, Vare PO, Melkko J, Tuominen H, Tuppurainen K, Makela J, Karttunen TJ and Makinen MJ. Inflammation and prognosis in colorectal cancer. Eur J Cancer 2005; 41: 2645-2654.

[16] Galon J, Mlecnik B, Bindea G, Angell HK, Berger A, Lagorce C, Lugli A, Zlobec I, Hartmann A, Bifulco C, Nagtegaal ID, Palmqvist R, Masucci GV, Botti G, Tatangelo F, Delrio P, Maio M, Laghi L, Grizzi F, Asslaber M, D'Arrigo C, Vidal-Vanaclocha F, Zavadova E, Chouchane L, Ohashi PS, Hafezi-Bakhtiari S, Wouters BG, Roehrl M, Nguyen L, Kawakami Y, Hazama S, Okuno K, Ogino S, Gibbs P, Waring P, Sato N, Torigoe T, Itoh K, Patel PS, Shukla SN, Wang Y, Kopetz S, Sinicrope FA, Scripcariu V, Ascierto PA, Marincola FM, Fox BA and Pages F. Towards the introduction of the 'Immunoscore' in the classification of malignant tumours. J Pathol 2014; 232: 199-209.

[17] Zhang D, He W, Wu C, Tan Y, He Y, Xu B, Chen L, Li Q and Jiang J. Scoring system for tumor-infiltrating lymphocytes and its prognostic value for gastric cancer. Front Immunol 2019; 10: 71.

[18] Hendry S, Salgado R, Gevaert T, Russell PA, John T, Thapa B, Christie M, van de Vijver K, Estrada MV, Gonzalez-Ericsson PI, Sanders M, Solomon B, Solinas C, Van den Eynden GGGM, Allory Y, Preusser M, Hainfellner J, Pruneri G,

Vingiani A, Demaria S, Symmans F, Nuciforo P, Comerma L, Thompson EA, Lakhani S, Kim SR, Schnitt S, Colpaert C, Sotiriou C, Scherer SJ, Ignatiadis M, Badve S, Pierce RH, Viale G, Sirtaine N, Penault-Llorca F, Sugie T, Fineberg S, Paik S, Srinivasan A, Richardson A, Wang Y, Chmielik E, Brock J, Johnson DB, Balko J, Wienert S, Bossuyt V, Michiels S, Ternes N, Burchardi N, Luen SJ, Savas P, Klauschen F, Watson PH, Nelson BH, Criscitiello C, O'Toole S, Larsimont D, de Wind R, Curigliano G, Andre F, Lacroix-Triki M, van de Vijver M, Rojo F, Floris G, Bedri S, Sparano J, Rimm D, Nielsen T, Kos Z, Hewitt S, Singh B, Farshid G, Loibl S, Allison KH, Tung N, Adams S, Willard-Gallo K, Horlings HM, Gandhi L, Moreira A, Hirsch F, Dieci MV, Urbanowicz M, Brcic I, Korski K, Gaire F, Koeppen H, Lo A, Giltnane J, Rebelatto MC, Steele KE, Zha J, Emancipator K, Juco JW, Denkert C, Reis-Filho J, Loi S and Fox SB. Assessing tumor-infiltrating lymphocytes in solid tumors: a practical review for pathologists and proposal for a standardized method from the international immunooncology biomarkers working group: part 1: assessing the host immune response, TILs in invasive breast carcinoma and ductal carcinoma in situ, metastatic tumor deposits and areas for further research. Adv Anat Pathol 2017; 24: 235-251.

[19] Shinkawa T, Ohuchida K, Mochida Y, Sakihama K, Iwamoto C, Abe T, Ideno N, Mizuuchi Y, Shindo K, Ikenaga N, Moriyama T, Nakata K, Oda Y and Nakamura M. Subtypes in pancreatic ductal adenocarcinoma based on niche factor dependency show distinct drug treatment responses. J Exp Clin Cancer Res 2022; 41: 89.

[20] Husstegge M, Hoang NA, Rebstock J, Monecke A, Gockel I, Weimann A, Schumacher G, Bechmann I, Lordick F, Kallendrusch S and Korfer J. PD-1 inhibition in patient derived tissue cultures of human gastric and gastroesophageal adenocarcinoma. Oncoimmunology 2021; 10: 1960729.

[21] Valanciute A, Mathieson L, O'Connor RA, Scott JI, Vendrell M, Dorward DA, Akram AR and Dhaliwal K. Phototherapeutic induction of immunogenic cell death and CD8+ T cell-granzyme B mediated cytolysis in human lung cancer cells and organoids. Cancers (Basel) 2022; 14: 4119.

[22] Salgado R, Denkert C, Demaria S, Sirtaine N, Klauschen F, Pruneri G, Wienert S, Van den Eynden G, Baehner FL, Penault-Llorca F, Perez EA, Thompson EA, Symmans WF, Richardson AL, Brock J, Criscitiello C, Bailey H, Ignatiadis M, Floris G, Sparano J, Kos Z, Nielsen T, Rimm DL, Allison KH, Reis-Filho JS, Loibl S, Sotiriou C, Viale G, Badve S, Adams S, Willard-Gallo K and Loi S; International TILs Working Group 2014. The evaluation of tumor-infiltrating lymphocytes (TILs) in breast cancer: recommendations by an International TILs Working Group 2014. Ann Oncol 2015; 26: 259-271.

[23] Thagaard J, Broeckx G, Page DB, Jahangir CA, Verbandt S, Kos Z, Gupta R, Khiroya R, Abduljabbar K, Acosta Haab G, Acs B, Akturk G, Almeida JS, Alvarado-Cabrero I, Amgad M, Azmoudeh-Ardalan F, Badve S, Baharun NB, Balslev E, Bellolio ER, Bheemaraju V, Blenman KR, Botinelly Mendonca Fujimoto L, Bouchmaa N, Burgues O, Chardas A, Chon U Cheang M, Ciompi F, Cooper LA, Coosemans A, Corredor G, Dahl AB, Dantas Portela FL, Deman F, Demaria S, Dore Hansen J, Dudgeon SN, Ebstrup T, Elghazawy M, Fernandez-Martin C, Fox SB, Gallagher WM, Giltnane JM, Gnjatic S, Gonzalez-Ericsson PI, Grigoriadis A, Halama N, Hanna MG, Harbhajanka A, Hart SN, Hartman J, Hauberg S, Hewitt S, Hida AI, Horlings HM, Husain Z, Hytopoulos E, Irshad S, Janssen EA, Kahila M, Kataoka TR, Kawaguchi K, Kharidehal D, Khramtsov AI, Kiraz U, Kirtani P, Kodach LL, Korski K, Kovacs A, Laenkholm AV, Lang-Schwarz C, Larsimont D, Lennerz JK, Lerousseau M, Li X, Ly A, Madabhushi A, Maley SK, Manur Narasimhamurthy V, Marks DK, McDonald ES, Mehrotra R, Michiels S, Minhas FUAA, Mittal S, Moore DA, Mushtaq S, Nighat H, Papathomas T, Penault-Llorca F, Perera RD, Pinard CJ, Pinto-Cardenas JC, Pruneri G, Pusztai L, Rahman A, Rajpoot NM, Rapoport BL, Rau TT, Reis-Filho JS, Ribeiro JM, Rimm D, Roslind A, Vincent-Salomon A, Salto-Tellez M, Saltz J, Sayed S, Scott E, Siziopikou KP, Sotiriou C, Stenzinger A, Sughayer MA, Sur D, Fineberg S, Symmans F, Tanaka S, Taxter T, Tejpar S, Teuwen J, Thompson EA, Tramm T, Tran WT, van der Laak J, van Diest PJ, Verghese GE, Viale G, Vieth M, Wahab N, Walter T, Waumans Y, Wen HY, Yang W, Yuan Y, Zin RM, Adams S, Bartlett J, Loibl S, Denkert C, Savas P, Loi S, Salgado R and Specht Stovgaard E. Pitfalls in machine learning-based assessment of tumor-infiltrating lymphocytes in breast cancer: a report of the international immuno-oncology biomarker working group on breast cancer. J Pathol 2023; 260: 498-513.

[24] Maibach F, Sadozai H, Seyed Jafari SM, Hunger RE and Schenk M. Tumor-infiltrating lymphocytes and their prognostic value in cutaneous melanoma. Front Immunol 2020; 11: 2105.

[25] Chatziioannou E, Rossner J, Aung TN, Rimm DL, Niessner H, Keim U, Serna-Higuita LM, Bonzheim I, Kuhn Cuellar L, Westphal D, Steininger J, Meier F, Pop OT, Forchhammer S, Flatz L, Eigentler T, Garbe C, Rocken M, Amaral T and Sinnberg T. Deep learning-based scoring

of tumour-infiltrating lymphocytes is prognostic in primary melanoma and predictive to PD-1 checkpoint inhibition in melanoma metastases. EBioMedicine 2023; 93: 104644.
[26] Stumpf M, Hasenburg A, Riener MO, Jutting U, Wang C, Shen Y, Orlowska-Volk M, Fisch P, Wang Z, Gitsch G, Werner M and Lassmann S. Intraepithelial CD8-positive T lymphocytes predict survival for patients with serous stage III ovarian carcinomas: relevance of clonal selection of T lymphocytes. Br J Cancer 2009; 101: 1513-1521.
[27] Stout A, Facey N, Bhatnagar A, Rice K, Berditchevski F, Kearns D, Metcalf A, Elghobashy A and Shaaban AM. Profiling of tumour-infiltrating lymphocytes and tumour-associated macrophages in ovarian epithelial cancer-relation to tumour characteristics and impact on prognosis. Int J Mol Sci 2024; 25: 4524.
[28] Dong J, Li J, Liu SM, Feng XY, Chen S, Chen YB and Zhang XS. CD33(+)/p-STAT1(+) double-positive cell as a prognostic factor for stage IIIa gastric cancer. Med Oncol 2013; 30: 442.
[29] Arigami T, Uenosono Y, Ishigami S, Matsushita D, Hirahara T, Yanagita S, Okumura H, Uchikado Y, Nakajo A, Kijima Y and Natsugoe S. Decreased density of CD3+ tumor-infiltrating lymphocytes during gastric cancer progression. J Gastroenterol Hepatol 2014; 29: 1435-1441.
[30] Liu K, Yang K, Wu B, Chen H, Chen X, Chen X, Jiang L, Ye F, He D, Lu Z, Xue L, Zhang W, Li Q, Zhou Z, Mo X and Hu J. Tumor-infiltrating immune cells are associated with prognosis of gastric cancer. Medicine (Baltimore) 2015; 94: e1631.
[31] Kang BW, Seo AN, Yoon S, Bae HI, Jeon SW, Kwon OK, Chung HY, Yu W, Kang H and Kim JG. Prognostic value of tumor-infiltrating lymphocytes in Epstein-Barr virus-associated gastric cancer. Ann Oncol 2016; 27: 494-501.
[32] Li Q, Zhang D, He W, Chen T, Yan Z, Gao X, Chen L, Zheng X, Xu B, Lu B and Jiang J. CD8(+) T cells located in tertiary lymphoid structures are associated with improved prognosis in patients with gastric cancer. Oncol Lett 2020; 20: 2655-2664.
[33] Lee JS, Won HS, Sun S, Hong JH and Ko YH. Prognostic role of tumor-infiltrating lymphocytes in gastric cancer: a systematic review and meta-analysis. Medicine (Baltimore) 2018; 97: e11769.
[34] Philip M and Schietinger A. CD8(+) T cell differentiation and dysfunction in cancer. Nat Rev Immunol 2022; 22: 209-223.
[35] Espinosa-Carrasco G, Chiu E, Scrivo A, Zumbo P, Dave A, Betel D, Kang SW, Jang HJ, Hellmann MD, Burt BM, Lee HS and Schietinger A. Intratumoral immune triads are required for immunotherapy-mediated elimination of solid tumors. Cancer Cell 2024; 42: 1202-1216, e1208.
[36] Meiser P, Knolle MA, Hirschberger A, de Almeida GP, Bayerl F, Lacher S, Pedde AM, Flommersfeld S, Honninger J, Stark L, Stogbauer F, Anton M, Wirth M, Wohlleber D, Steiger K, Buchholz VR, Wollenberg B, Zielinski CE, Braren R, Rueckert D, Knolle PA, Kaissis G and Bottcher JP. A distinct stimulatory cDC1 subpopulation amplifies CD8(+) T cell responses in tumors for protective anti-cancer immunity. Cancer Cell 2023; 41: 1498-1515, e1410.
[37] Moreno Ayala MA, Campbell TF, Zhang C, Dahan N, Bockman A, Prakash V, Feng L, Sher T and DuPage M. CXCR3 expression in regulatory T cells drives interactions with type I dendritic cells in tumors to restrict CD8(+) T cell antitumor immunity. Immunity 2023; 56: 1613-1630, e1615.
[38] Basak U, Sarkar T, Mukherjee S, Chakraborty S, Dutta A, Dutta S, Nayak D, Kaushik S, Das T and Sa G. Tumor-associated macrophages: an effective player of the tumor microenvironment. Front Immunol 2023; 14: 1295257.
[39] Lampiasi N. New strategies for macrophage reeducation in cancer: an update. Int J Mol Sci 2024; 25: 3414.
[40] Nagase H, Takeoka T, Urakawa S, Morimoto-Okazawa A, Kawashima A, Iwahori K, Takiguchi S, Nishikawa H, Sato E, Sakaguchi S, Mori M, Doki Y and Wada H. ICOS(+) Foxp3(+) TILs in gastric cancer are prognostic markers and effector regulatory T cells associated with Helicobacter pylori. Int J Cancer 2017; 140: 686-695.
[41] Gong LP, Chen JN, Xiao L, He Q, Feng ZY, Zhang ZG, Liu JP, Wei HB and Shao CK. The implication of tumor-infiltrating lymphocytes in Epstein-Barr virus-associated gastric carcinoma. Hum Pathol 2019; 85: 82-91.
[42] Shin SJ, Kim SY, Choi YY, Son T, Cheong JH, Hyung WJ, Noh SH, Park CG and Kim HI. Mismatch repair status of gastric cancer and its association with the local and systemic immune response. Oncologist 2019; 24: e835-e844.
[43] Ma W, Li W, Xu L, Liu L, Xia Y, Yang L and Da M. Identification of a gene prognostic model of gastric cancer based on analysis of tumor mutation burden. Pathol Oncol Res 2021; 27: 1609852.
[44] Wang D, Wang N, Li X, Chen X, Shen B, Zhu D, Zhu L, Xu Y, Yu Y and Shu Y. Tumor mutation burden as a biomarker in resected gastric cancer via its association with immune infiltration and hypoxia. Gastric Cancer 2021; 24: 823-834.
[45] Castaneda C, Castillo M, Bernabe L, Suarez N, Fassan M, Sanchez J, Tello K, Alatrista R,

Chavez I, Ruiz E, Bazan Y, Barreda F, Valdivia D, Meng W, Chakravarti A, Sanchez J, Taxa L and Montenegro P. The relationship between tumour infiltrating lymphocytes, Epstein-Barr virus and Helicobacter pylori infection in gastric cancer. Ecancermedicalscience 2022; 16: 1362.

[46] Pereira MA, Ramos MFKP, Cardili L, de Moraes RDR, Dias AR, Szor DJ, Zilberstein B, Alves VAF, de Mello ES and Ribeiro U Jr. Prognostic implications of tumor-infiltrating lymphocytes within the tumor microenvironment in gastric cancer. J Gastrointest Surg 2024; 28: 151-157.

[47] Tian C, Jing H, Wang C, Wang W, Cui Y, Chen J and Sha D. Prognostic role of tumour-infiltrating lymphocytes assessed by H&E-stained section in gastric cancer: a systematic review and meta-analysis. BMJ Open 2021; 11: e044163.

[48] Zhang N, Zhang G, Wang D, Liu H, Zhang Y, Ayarick VA, Han X, Lv Y and Wang Y. The relationship of the tertiary lymphoid structures with the tumor-infiltrating lymphocytes and its prognostic value in gastric cancer. Arch Med Sci 2021; 20: 255-266.

[49] Ikeguchi M, Miyake T, Matsunaga T, Yamamoto M, Fukumoto Y, Yamada Y, Fukuda K, Saito H, Tatebe S and Tsujitani S. Recent results of therapy for scirrhous gastric cancer. Surg Today 2009; 39: 290-294.

[50] Ikeguchi M, Yamamoto O and Kaibara N. Management protocol for scirrhous gastric cancer. In Vivo 2004; 18: 577-580.

[51] Jinushi R, Mizuide M, Tanisaka Y, Masuda S, Koizumi K, Sasaki A, Ishihara Y, Shionoya K, Sato R, Sugimoto K, Shin T, Shiomi R, Fujita A, Ryozawa S and Yamazaki T. Efficacy for diagnoses of scirrhous gastric cancer and safety of endoscopic ultrasound-guided fine-needle aspiration: a systematic review and meta-analysis. JGH Open 2023; 7: 403-409.

[52] Hou W, Zhao Y and Zhu H. Predictive biomarkers for immunotherapy in gastric cancer: current status and emerging prospects. Int J Mol Sci 2023; 24: 15321.

[53] Cattaneo CM, Dijkstra KK, Fanchi LF, Kelderman S, Kaing S, van Rooij N, van den Brink S, Schumacher TN and Voest EE. Tumor organoid-T-cell coculture systems. Nat Protoc 2020; 15: 15-39.

[54] Olivo Pimentel V, Yaromina A, Marcus D, Dubois LJ and Lambin P. A novel co-culture assay to assess anti-tumor CD8(+) T cell cytotoxicity via luminescence and multicolor flow cytometry. J Immunol Methods 2020; 487: 112899.

[55] Jeong SR and Kang M. Exploring tumor-immune interactions in co-culture models of T cells and tumor organoids derived from patients. Int J Mol Sci 2023; 24: 14609.

[56] Buzza MS, Zamurs L, Sun J, Bird CH, Smith AI, Trapani JA, Froelich CJ, Nice EC and Bird PI. Extracellular matrix remodeling by human granzyme B via cleavage of vitronectin, fibronectin, and laminin. J Biol Chem 2005; 280: 23549-23558.

[57] Hendel A and Granville DJ. Granzyme B cleavage of fibronectin disrupts endothelial cell adhesion, migration and capillary tube formation. Matrix Biol 2013; 32: 14-22.

[58] Thompson R and Cao X. Reassessing granzyme B: unveiling perforin-independent versatility in immune responses and therapeutic potentials. Front Immunol 2024; 15: 1392535.